

NASA Contractor Report 185156

# User's Guide to PMESH—A Grid-Generation Program for Single-Rotation and Counterrotation Advanced Turboprops

Saif A. Warsi

*Sverdrup Technology, Inc.*

*NASA Lewis Research Center Group*

*Cleveland, Ohio*

December 1989

Prepared for

Lewis Research Center

Under Contract NAS3-24105



National Aeronautics and  
Space Administration

(NASA-CR-185156) USER'S GUIDE TO PMESH: A  
GRID-GENERATION PROGRAM FOR SINGLE-ROTATION  
AND COUNTERROTATION ADVANCED TURBOPROPS  
Final Report (Sverdrup Technology) 25 p

CSCL 09B 63/60

N90-14783

Unclas  
0254513

.

.

.

.

.

.

.

.

# USER'S GUIDE TO PMESH – A GRID-GENERATION PROGRAM FOR SINGLE-ROTATION AND COUNTERROTATION ADVANCED TURBOPROPS

Saif A. Warsi  
Sverdrup Technology, Inc.  
NASA Lewis Research Center Group  
Cleveland, Ohio 44135

## ABSTRACT

This report presents a detailed operating manual for a grid-generation program that produces three-dimensional meshes for advanced turboprops (ATP). The code uses both algebraic and elliptic partial differential equation (PDE) methods to generate single-rotation and counterrotation H – or C – type meshes for the  $z - r$  planes and H – type for the  $z - \theta$  planes. The code allows easy specification of geometrical constraints (such as blade angle, location of bounding surfaces, etc.) and mesh-control parameters (point distribution near blades and nacelle, number of grid points desired, etc.), and it has good runtime diagnostics. This report provides an overview of the mesh-generation procedure, a sample input dataset with detailed explanation of all input, and example meshes.

## INTRODUCTION

Three-dimensional computational fluid dynamic codes require grids with suitable resolution and smoothness. These qualities are especially difficult to maintain because of the taper, twist, and sweep of realistic turboprop geometries. Grid resolution near shocks and in shear layers allows for complex fluid physics to be captured. Smoothness of the grid prevents truncation errors, arising from the discretization of the flow equations, from dominating the solution.

This report describes a code for generating three-dimensional grids for advanced turboprops. The code uses mainly algebraic methods such as (1) Ferguson's parametric cubic curves, (2) cubic splines, and (3) cubic curves to generate meshes. Elliptic partial differential equations (PDE's) are used for further smoothing in certain cases. The resulting meshes, regardless of whether H – or C-type, have in common a two-dimensional axisymmetric mesh (common  $z$  and  $r$  coordinates), only varying in the  $\theta$  coordinate within the passage. The resulting meshes may be written in a variety of formats to conform to the input required for different flow solvers. For example, for the Adamczyk average-passage code (ref. 1), a counterrotation mesh can be written so that each blade row has its own H-mesh which describes a full passage from inlet to exit with each respective mesh accounting for its own blade thickness while applying zero thickness to the neighboring blade row.

## GEOMETRY AND MESH-GENERATION DESCRIPTIONS

The generation of computational meshes for advanced turboprops consists of a number of steps. First the user-supplied nacelle and blade shapes, as well as geometrical and mesh quality constraints are read. From this input, the common two-dimensional axisymmetric mesh is created by using a series of parametric cubic curves, cubic splines, and, in the case of C-type meshes, by limited use of PDE's for further smoothing. Second, the resulting two-dimensional meshes are smoothed by using equal-weighted averaging. Third, the  $\theta$  – coordinate surfaces are generated, based on the  $\theta$  coordinates of the given blade and the user-specified blade angle. Finally, the mesh is interpolated to the periodic angle and written subject to user requirements.

The geometry for the blade and spinner is provided by the user. The spinner/hub shape is input as  $(z, r)$  pairs with  $z$  increasing monotonically from the spinner stagnation point or inlet surface, downstream to the outflow boundary. The data is in the same scale as the blade geometry.

The blade definition is given as blade sections specified on planes perpendicular to a stacking axis which is also the pitch-change axis (PCA). The sections (stations) are specified from near the hub to the tip with the distance along the stacking axis (rb) increasing monotonically. At a given station, the section is located with the local twist angle  $\Delta\beta$  (dbet) based on the blade angle at 75-percent blade radius  $\beta_{3/4}$  (beta34), leading-edge alignment (lea), face alignment (fa), and chord length (cl). The section shape is given in a normalized coordinate system (x/cl, ys/cl, yp/cl) with points on the suction and pressure surfaces from the leading edge to the trailing edge. Figures 1 and 2 describe this geometry.

The preceding parameters are used to convert the blade sections to a cylindrical coordinate system. Then, user-specified point distribution (with respect to uniform unit spacing) and the following hyperbolic tangent distribution are used to generate a distribution of normalized points. Let

$$A = \frac{\sqrt{\Delta s_2}}{\sqrt{\Delta s_1}}$$

$$B = \frac{1}{I\sqrt{\Delta s_2\Delta s_1}}$$

where  $I$  is the number of points and  $\Delta s_1, \Delta s_2$  are the fractions of uniform spacing. Solving the following nonlinear equation for  $\delta$

$$\frac{\sinh \delta}{\delta} = B$$

gives the unit-segment point distribution as

$$s(\xi) = \frac{u(\xi)}{A + (1 - A)u(\xi)}$$

where

$$u(\xi) = \frac{1}{2} \left\{ 1 + \frac{\tanh[\delta(\frac{\xi}{I} - \frac{1}{2})]}{\tanh(\frac{\delta}{2})} \right\}$$

and  $\xi$  varies from 0 to  $I$ . See reference 2.

By using this normalized distribution, the points on each blade section are redistributed axially. The sections are then converted to constant radial sections. The initial curve designs for the two-dimensional mesh are done with Ferguson's parametric cubic curves (ref. 3). These curves are defined as follows:

$$\mathbf{r} = \mathbf{r}(u) = \mathbf{a}_0 + u\mathbf{a}_1 + u^2\mathbf{a}_2 + u^3\mathbf{a}_3$$

where  $0 \leq u \leq 1$ .

To determine  $\mathbf{a}_0, \mathbf{a}_1, \mathbf{a}_2$ , and  $\mathbf{a}_3$ , specify the values of  $\mathbf{r}$  and  $d\mathbf{r}/du$  at both ends of the segments. Now, the  $\mathbf{a}$ 's in terms of the  $\mathbf{r}$ 's may be obtained in matrix form:

$$\mathbf{r}(u) = \begin{bmatrix} 1 & u & u^2 & u^3 \end{bmatrix} \begin{bmatrix} 1 & 0 & 0 & 0 \\ 0 & 0 & 1 & 0 \\ -3 & 3 & -2 & -1 \\ 2 & -2 & 1 & 1 \end{bmatrix} \begin{bmatrix} \mathbf{r}(0) \\ \mathbf{r}(1) \\ \dot{\mathbf{r}}(0) \\ \dot{\mathbf{r}}(1) \end{bmatrix}$$

The derivatives  $\dot{\mathbf{r}}(0)$  and  $\dot{\mathbf{r}}(1)$  are proportional to the unit tangent vectors  $\mathbf{T}(0)$  and  $\mathbf{T}(1)$  at the ends of the of the line segment under consideration. We may write

$$\dot{\mathbf{r}}(0) = \alpha_0 \mathbf{T}(0) \quad ; \quad \dot{\mathbf{r}}(1) = \alpha_1 \mathbf{T}(1)$$

By varying the tangent vector lengths, different-shaped curves are easily generated (fig. 3). These curves are used to smoothly splice the  $z$ - $r$  curves from the blades to each external boundary. Now the point distribution on the blades and the hyperbolic tangent distribution function generate a smooth distribution of points away from all solid surfaces. Cubic splines along with the new unit point distributions are used to obtain a very

smooth variation of  $z$  and  $r$  coordinates everywhere. In order to further smooth the  $z$  and  $r$  coordinates, an equal-weighted smoothing is applied. In C-type meshes, the redistribution scheme may cause a high degree of skewness in the cone region (the rounded region up to the leading edge of the blade). Elliptic PDE's are used to smooth this area (ref. 2). The basic differential equations under consideration are

$$\nabla^2 \xi = P$$

and

$$\nabla^2 \eta = Q$$

where  $\xi$ ,  $\eta$  are the coordinates in the uniform computational domain, and  $P$ ,  $Q$  are called the "control functions". These functions allow the user to control the placement of the grid points in the desired region. However, in this report, the equations solved were

$$\nabla^2 \xi = 0 \tag{1}$$

and

$$\nabla^2 \eta = \frac{g_{11}Q}{G} \tag{2}$$

Hence, the point distribution is controlled only in the  $\eta$  direction. However, the solution of equations 1 and 2 will yield a distribution of  $\xi$  and  $\eta$  which is known to be a uniform rectangular two-dimensional plane (fig. 4). Therefore, inverting equations 1 and 2 in order to change the role of the dependent and independent variables gives

$$g_{22}r_{\xi\xi} - 2g_{12}r_{\xi\eta} + g_{11}r_{\eta\eta} = -g_{11}Qr_{\eta} \tag{3}$$

where  $r$  is a vector of the physical coordinates  $z$ ,  $r$  and

$$g_{11} = z_{\xi}^2 + r_{\xi}^2$$

$$g_{12} = z_{\xi}z_{\eta} + r_{\xi}r_{\eta}$$

$$g_{22} = z_{\eta}^2 + r_{\eta}^2$$

and

$$G = (z_{\xi}r_{\eta} - z_{\eta}r_{\xi})^2$$

is known as the square of the Jacobian of transformation. The forcing function may be arbitrary, and the one chosen was

$$Q = \frac{-(2 + (\eta - 1) * \log(\chi)) * \log(\chi)}{1. + (\eta - 1) * \log(\chi)}$$

This function will allow the user to increase the grid clustering near the  $\eta = 0$  boundary with increasing  $\chi$  ( $\chi \geq 1$ ). Equations 3 are first discretized on the computational plane by central differences and then solved with a block relaxation scheme where the block was a line in this case (Line SOR).

Two appendixes are provided to guide the user in the proper use of this program. Appendix A lists and explains, in detail, all inputs required; appendix B provides a typical input dataset.

## RESULTS

Figures 5 to 8 show different views of a counterrotation H-mesh generated by using the attached example dataset with JNOSE changed to 8. Figure 5 shows a view of the  $z-r$  plane; notice the effect of the clustering factors near the nacelle, tip, and at the edges of the blades. Figures 6(a) and 6(b) show the effect of the clustering factors (DZLE, DZTE, DZLE2, and DZTE2) on the blade point distribution. DZLE and DZTE were changed to 0.5 and 1.0, respectively, for the front blade. Their effect can be seen clearly in figure 6(b). Figure 7 shows a portion of a full passage via a radial cut at the hub, with the axial index starting just a few gridlines ahead of the front blade and finishing a few gridlines aft of the rear blade.

Figure 8(a) shows the full passage view for a single blade case via a radial cut at the hub. In this case, DTHBL was 0.2; DTHBL was then changed to 1.0. The effect of this change is seen in figure 8(b). Figures 9(a) and 9(b) show a constant axial cut at the inlet and at approximately midchord of the blade, respectively.

Figure 10 shows an example C-mesh. To generate this mesh, the nacelle input was changed to have no sting, CONOPT was changed to True, JCONE was set, and CK was set to 1.1.

Finally, Figure 11 shows the surface meshes for a swirl-recovery vane (SRV) grid, a cruise missile (CM) and an advanced single-rotation turboprop (ATP).

## CONCLUSIONS

An algebraic and elliptic partial differential equation mesh generator has been developed for generation of three-dimensional meshes for advanced turboprops and other similar geometries. H- and C-type meshes may be generated for both single-rotation and counterrotation cases. The program has good runtime diagnostics, and the user may easily modify the mesh-control parameters.

## ACKNOWLEDGEMENTS

The author would like to thank Dr. Christopher J. Miller for his valuable contributions to the debugging and development of this code. The surface grid figures for this report were also produced by Dr. Miller.

## APPENDIX A

### USER'S MANUAL FOR THE ADVANCED TURBOPROP MESH GENERATOR

The mesh generator is coded in FORTRAN 77 with 34 subroutines and 2 external functions. The code has been run on a wide variety of computer systems with no coding changes. Figure 12 shows a flow chart of the main program structure.

The nacelle and blade geometries, the mesh size and spacing parameters, and the controls for miscellaneous options are all read from FORTRAN UNIT 7 in the following formats: (1) The majority of real number fields are read in F10.5 format, while a few are read in free-format (F-F), (2) integers are read using an I5 format, and (3) logical fields are read in L5 format. In order for the program to operate, the input file must be named "fort.7". The uppercase lines shown in the following description of the sample input serve as comments and are skipped over by the program; however, they must be included in the input for proper operation. All actual input lines are listed in their lowercase alphanumeric form. An explanation of all input follows the sample. Appendix B shows a sample input dataset for a counterrotation case.

title      There may be as many lines of text in the title section as the user desires. The only restriction is that the following line with "PT10" must exist. Note that the leading space in "PT10" is significant. The title is read with an "A" format; the maximum length of each line is 80 characters.

PT10 PT20 PT30 PT40 PT50 - (5L5)

pt10 pt20 pt30 pt40 pt50      These are logical flags which are read with a (5L5) format. The print flags (following) print all the coordinates ( $z, r, \theta$ ); if PT30 or PT40 has been invoked, ignore the  $\theta$  coordinates. Until subroutine EXTEND has been called, only the  $\theta$  on the blades are correct. When any flag is True, the program will print the following:

pt10      Print all input, as well as the blade geometry or geometries (if two blade rows) in normalized (diameter = 1.) cylindrical form; see subroutine MEREAD.

pt20      Print blade(s) after correct axial distribution is applied and the stations are at constant radius; see subroutine ADJBLD. Also print the fictitious base coordinates; see subroutine FICBAS.

pt30      Print the regions comprising the rest of the surface through the blade(s); see subroutines FORBLD and MIDBLD (used only when generating two blade rows), OUTREG, and CONREG.

pt40      Print the blade surface after radial distribution is applied; see subroutine RADJST and then after the surface not on the blade(s) is smoothed, see subroutines AVGSRF and AVG.

pt50      Print the entire, final mesh after all other processing; see subroutine MWRITE. This produces hundreds of pages of mostly useless output. Use this option only when necessary.

COUNTER-ROTATION - (L5)

cropt      Logical counterrotation option flag. Use an L5 format to read. If True, then two blade geometries will be read from the input, first the front and then the rear. If False, then single rotation is selected.

NACELLE GEOMETRY

NUMBER OF INPUT STATIONS FOR NACELLE - (I5)

nn      Number of points specified on the nacelle.

zn(1),rn(1) to zn(nn),rn(nn)      The actual nacelle geometry, from the nose or any extension, such as a sting for an H-mesh (1) back to somewhere behind the blade (nn). The pitch-change axis (PCA) of the (front) blade is used as the axial  $z$  origin; upstream of the PCA (toward the nose) is negative. The rotation axis is, of course, the origin radially  $r$ . The nacelle geometry should be in the same scale as the blade geometry(s). The nacelle geometry is read in a 2F10.5 format.

## BLADE GEOMETRY

BL.DIA. BETA34 NR NC - (2F10.5,2I5)

diam The diameter of the blade. Everything is scaled by the program so that the working diameter of the (front) blade is 1. in the output mesh.

beta34 The value of beta at 75-percent radius. Beta is the angle, in a given plane normal to the PCA, between the chord line and the plane of rotation.

nr Number of radial stations in the input. This can be different for the two blade rows, if the user is generating a counterrotation grid. The input stations should not include a fictitious station of data at  $rb = 0$  (see following for definition of  $rb$ ). Station  $nr$  is at the tip.

nc Number of stations along the chord line at each blade cross-section in the input. Station 1 is the leading edge and station  $nc$  is the trailing edge.

RB DBETA LEA FA CL - (5F10.5)  
X YS YP X YS YP - (10X,6F10.5)

rb The distance from the rotational axis to the plane containing the current blade section. This should be in the same units as diameter.

dbet The angle, in degrees, to be added to beta34 to get the value of beta for the current station. see beta34.

lea Leading-edge alignment. The distance along the chord line from the point on the chord line closest to the PCA to the leading edge; lea is positive if the point closest to the PCA is aft of the leading edge. Same units as diameter.

fa Face alignment. The perpendicular distance from the PCA to the chord line of the current station; fa is positive if the PCA is on the face (pressure) side. Same units as diameter.

cl The chord length (from leading to trailing edge) at the current station. The following blade coordinates are nondimensionalized by this value. Same units as diameter.

x(i),ys(i),yp(i) The blade shape at the current station. Where  $x$  is the fractional chordwise distance (0.0:leading edge to 1.0:trailing edge) and  $(ys, yp)$  are the distances perpendicular to the chord line, normalized by the chord length. The blade section may be input with a finite thickness at the leading and trailing edges; the program will, however, force the thickness to be zero at the leading and trailing edges. The (face/lower/pressure) surface is defined by  $yp$ , while the (camber/upper/suction) surface is defined by  $ys$ . Note that data for two  $x$  values are on each input line.

## MESH PARAMETERS

ZUP ZDN RINF - (3F10.5)

zup The upstream boundary of the mesh, measured axially from the PCA in fractions of a diameter. It is in a scale where the blade diameter is 1.0; hence, if the input blade diameter changes this should stay the same to get the same relative location. It has to be negative. Note that for an H-mesh,  $zup$  must not be beyond the upstream limit of the nacelle input.

zdn The downstream boundary of the mesh. Scaled the same as  $zup$ . If it is beyond the downstream limit of the nacelle input, the nacelle will be extended straight back (at the same radius) from its last station.

rinf The radial boundary of the mesh. If there is no outer region, i.e.,  $kmax = ktip$  (see  $kmax$ ), this will be ignored, and 0.5 (the normalized tip radius) will be used instead. It is scaled the same as  $zup$  and has to be  $\geq 0.5$  when used.



#### CONE FLAG - (L5)

conopt      This is the cone option flag. If True, then the cone region (if present; see jcone) will have a curved outer boundary (C-mesh nose). If False, then the region will have a rectangular boundary (H-mesh).

#### JCONE JLE JSL JTE JMAX KTIP KMAX LMAX - (8I5)

jcone      The location of cone region. J is the index in the axial direction; jcone specifies the number of axial stations in the cone region. If it is zero, there will be no cone region; otherwise, it should be at least 3.

jle      Index of the leading edge of the blade. The region from jcone to jle is called the "fore region", so jle must be greater than jcone.

jsl      Index of the shock line clustering on the (front) blade. If this is zero, there will be no clustering. See dzsl and cfsl.

jte      Index of the trailing edge of the (front) blade. If generating a single-rotation grid, the region from here to jmax is the aft region; otherwise, from here to jle2 (leading-edge index of (second) blade row) is the midregion.

jmax      Index of the downstream limit of the mesh ( $z = z_{dn}$ ). J is the axial index.

ktip      Index of the tip of the blade. K is the radial index. The region from 1 to ktip is the region from the rotation axis to the blade tip.

kmax      Index of the outer boundary of the mesh. From ktip to kmax is the outer region (excluding the part upstream of jcone, which is in the cone region). If  $kmax = ktip$ , there is no outer region and the tip radius will be the maximum radius instead of rinf.

lmax      Number of stations in the circumferential direction. l increases as  $\theta$  increases.

#### NBLADE - (I5)

nb      The number of blades on the front row.

#### LOCATE ZLEINF ZTEINF - (L5,2F10.5)

locflg      Logical flag which, when True, will use zleinf and zteinf for the specification of the leading- and trailing- edge extensions at the outer boundary.

zleinf      If locflg is True, this specifies, in the units used for zup, the axial location of the extension of the leading edge at rinf. It must be less than  $z_{dn}$  and greater than zup. If there is a cone region, it also should be greater than the scaled-down location of the nacelle nose ( $z_{n(1)}/diam$ ).

zteinf      Same as zleinf, but for the trailing edge. Must be greater than zleinf and less than ( $z_{n(n)}/diam$ ).

#### DZLE DZSL DZTE CFSL DRNAC DRTIP DTHBL - (F-F)

dzle      The mesh-clustering factor in the axial direction at the leading edge of the (front) blade. This is the fraction of an even spacing on the blade. If it is 1.0, the leading edge will have no clustering, while if it is 0.1, the mesh will be approximately 10 times denser at the leading edge (compared to uniform unit spacing).

dzsl      Clustering factor for the shockline on the (front) blade, if jsl is not zero. See cfsl.

dzte      Clustering factor for the trailing edge of the (front) blade.

cfsl      If the shock-line clustering is selected (jsl is not zero), the location of the clustering on the blade is given. cfsl stands for chord fraction at the shock line; consequently, if the chord fraction is 0.2, the clustering will be one-fifth the distance from the leading edge back to the trailing edge (closer to the leading edge).

drnac      Clustering factor in the radial direction at the nacelle surface. In the cone region this also gives a compression axially in front of the nose.

drtip      Clustering factor in the radial direction at the blade tip. It is phased out in the fore region so that it has no effect in the cone region.

dthbl      Clustering factor in the circumferential direction at the blade surfaces (and their axial and radial extensions).

#### ZREAR    REFL - (F10.5,L5)

zrear      If the user is generating a counterrotation mesh, this specifies the location of the rear PCA with respect to the front. Same units as diameter. This has to be greater than 0.

reflag      Logical flag for counterrotation. If True, the rear blade geometry will be reflected about  $\theta = 0$ . before being used. If the front and rear blades have the same shape (i.e., identical input), only reflected, the front geometry can be copied and this flag set. If the ys (suction side) input values are greater than the yp values, then this option should be used. Plots of the resulting mesh can also be used as guides to determine when to use this option.

The rest of the input is very similar to the input for the front blade. Some of the variables have a "2" appended to their names which indicates that the variables pertain to the rear blade row. The only difference that should be noted is that the rear blade is scaled down by the front blade diameter for consistency of units. This means that the rear blade tip will not necessarily be at  $r/d = 0.5$ . The user is cautioned that at this time the option to specify the leading- and trailing- edge extension locations for the rear blade should not be used ( it may cause problems); therefore, set locfl2 = False. From the input it may be interpreted that the number of blades on the rear row and the number of theta stations in a passage may be different than the number from the front. Please note that this is not a general change, because the subroutine MWRITE is now very much flow-solver specific. This change is valid only for the Adamczyk flow-solver format because it will output two mesh files; one with thickness for the front row and no rear blade thickness and the other with no thickness for the front row and with thickness for the rear blade. See the flag IPRNT.

#### JNOSE - (F-F)

jnose      If an II-mesh is being generated, then an axial index (jnose) value for the location of the stagnation point is read. This helps maintain the original nacelle shape as specified by the input. if jnose is specified as 0, then a value of jnose is computed as half of the leading-edge index (jle). If jnose is greater than 0, then it is taken to be the index desired ( must be greater than 3). If jnose is specified as less than 0, then the points are distributed axially from  $j=1$  to  $jle$ , and no stagnation point is preserved. This is important for certain types of nacelle bodies that do not have a stagnation point as such. One can also set jnose less than 0 for bodies that do have a stagnation point, however, the stagnation point will be faired out. if jnose is set greater than or equal to 0 for a body with no stagnation point, the code will not run properly.

#### CK C-MESH POISSON SMOOTHING PARAMETER ; < 0 NO SMOOTHING) - (F-F)

ck      Used only for a C-type mesh. This is a factor used to pack points above the tip. Values of ck should range from 1. to 2. Since the Poisson smoothing only operates from  $k_{tip}+1$  to  $k_{max}$  and  $j = 1$  to  $j_{cone}+1$ , the effect of higher ck is to pack more points near  $k_{tip}+1$ . A value of  $ck = 1$  will give a solution of the Laplace equation. If the mesh appears to have skewness near the leading-edge index above the tip without smoothing, then turn on the smoothing; try an initial value of  $ck = 1.15$ . Higher values will cause more line contraction near the  $k_{tip}+1$  line.

#### IPRNT MESH OUTPUT WRITE FLAG - (F-F)

iprnt - This flag controls the format of the mesh as it is written. IPRNT = 1 will write a mesh formatted for NASPROP-E (ref. 4), IPRNT = 2 writes a mesh formatted for the DENTON code (ref. 5), and IPRNT = 3 writes a mesh formatted for the ADAMCZYK codes (ref. 1). See subroutine MWRITE for actual write statements.

#### RAT (CIRCUMFERENTIAL PACKING RATIO; USED IF $\geq 1$ ) - (F-F)

rat - This a circumferential clustering factor. If rat is greater than or equal to 1 then rat will be used for the clustering in the  $\theta$  direction. This will overwrite any effect of the dthbl factor given previously. A value of rat equal to 1 will give uniform spacing; even small increases in rat (i.e. 0.1 or less) will change the packing considerably. In order to use rat, the number of desired mesh points in the circumferential direction must be odd; i.e., lmax has to be odd. However, if lmax has been specified as even, the program will change lmax to odd. A message informing the user of the change will be written to UNIT 6. See dthbl which also does packing in the circumferential direction. When dthbl is specified, a hyperbolic tangent stretching is performed; using rat gives a stretching based on series summation.

### OUTPUT

UNIT 6 is the debugging output; the print flags (pt10, pt20 , etc.) control what is printed, and informational messages (whether error or otherwise) are written here. Also written to UNIT 6 is the header page and any text that the user placed in the title portion of the input file. The output should be self-explanatory. UNIT 11 (and perhaps also UNIT 12, if generating a counterrotation mesh for the Adamczyk flow-solver) is the final output (mesh). Please note that the final output file or files are always named "fort.11" and "fort.12". Files by these names should not exist before the mesh generation process because the program will abort prematurely. The output files are unformatted. The first record contains the size and location parameters and has two forms depending upon whether it is a single-rotation or counterrotation mesh. The actual mesh coordinates are then written. See subroutine MWRITE for the actual write statements since they will vary depending upon the flag IPRNT. However, all write so that the  $z$ , then  $r$ , and finally, the  $\theta$  (in radians) coordinates are written.

# APPENDIX B SAMPLE INPUT DATASET

> This is a sample input dataset for generating a H-Mesh Counter-rotation  
> Advanced Turboprop grid.  
>  
> To convert to a single blade row, edit the dataset so that data  
> from the comment LOCATION REPT up to but not including the comment  
> JMOSE is deleted.  
>

> To convert to a C-Mesh, edit the nacelle geometry so that it has no  
> sting. Then change COM2 FLAG to True and JCOM2 between 3 and JLE.  
> This will create a Counter-rotation C-Mesh. For a single rotation  
> C-Mesh, make same change as above to convert to single blade row.

PTID PT20 PT30 PT40 PT50  
F F F F F  
COUNTER-ROTATION FLAG  
T  
MACELLZ GEOMETRY  
NUMBER OF INPUT STATIONS FOR MACELLZ  
66

Z  
-20.0000 0.0000  
-1.0000 0.0000  
-0.2980 0.0000  
-0.2970 0.0000  
-0.295920 0.000000  
-0.2958 0.0025  
-0.2950 0.0050  
-0.287760 0.014857  
-0.279590 0.022857  
-0.271420 0.029796  
-0.251020 0.043673  
-0.230610 0.055102  
-0.189800 0.073469  
-0.148900 0.088163  
-0.108160 0.100820  
-0.104490 0.101840  
-0.107040 0.102450  
-0.091837 0.104900  
-0.081633 0.106120  
-0.063265 0.105920  
-0.061224 0.105710  
-0.051020 0.105920  
-0.040816 0.107550  
-0.030612 0.110000  
-0.020408 0.112860  
-0.010204 0.116120  
0.000000 0.119510  
0.006122 0.121670  
0.018367 0.126040  
0.030612 0.130610  
0.042857 0.136780  
0.055102 0.139140  
0.067347 0.143510  
0.079592 0.147800  
0.091837 0.152240  
0.092857 0.152690  
0.095918 0.153710  
0.100000 0.154900  
0.104000 0.156450  
0.108160 0.157710  
0.112240 0.159980  
0.116330 0.160160  
0.120410 0.161270  
0.124490 0.162410  
0.128570 0.163390  
0.132650 0.164370  
0.136730 0.165220  
0.140810 0.165910  
0.144890 0.166810  
0.148970 0.167240  
0.153050 0.167290  
0.157130 0.167310  
0.161210 0.167350  
0.165290 0.167350  
0.169370 0.167350  
0.173450 0.167350  
0.177530 0.167350  
0.181610 0.167350  
0.185690 0.167350  
0.189770 0.167350  
0.193850 0.167350  
0.197930 0.167350  
0.202010 0.167350  
0.206090 0.167350  
0.210170 0.167350  
0.214250 0.167350  
0.218330 0.167350  
0.222410 0.167350  
0.226490 0.167350  
0.230570 0.167350  
0.234650 0.167350  
0.238730 0.167350  
0.242810 0.167350  
0.246890 0.167350  
0.250970 0.167350  
0.255050 0.167350  
0.259130 0.167350  
0.263210 0.167350  
0.267290 0.167350  
0.271370 0.167350  
0.275450 0.167350  
0.279530 0.167350  
0.283610 0.167350  
0.287690 0.167350  
0.291770 0.167350  
0.295850 0.167350  
0.299930 0.167350  
0.304010 0.167350  
0.308090 0.167350  
0.312170 0.167350  
0.316250 0.167350  
0.320330 0.167350  
0.324410 0.167350  
0.328490 0.167350  
0.332570 0.167350  
0.336650 0.167350  
0.340730 0.167350  
0.344810 0.167350  
0.348890 0.167350  
0.352970 0.167350  
0.357050 0.167350  
0.361130 0.167350  
0.365210 0.167350  
0.369290 0.167350  
0.373370 0.167350  
0.377450 0.167350  
0.381530 0.167350  
0.385610 0.167350  
0.389690 0.167350  
0.393770 0.167350  
0.397850 0.167350  
0.401930 0.167350  
0.406010 0.167350  
0.410090 0.167350  
0.414170 0.167350  
0.418250 0.167350  
0.422330 0.167350  
0.426410 0.167350  
0.430490 0.167350  
0.434570 0.167350  
0.438650 0.167350  
0.442730 0.167350  
0.446810 0.167350  
0.450890 0.167350  
0.454970 0.167350  
0.459050 0.167350  
0.463130 0.167350  
0.467210 0.167350  
0.471290 0.167350  
0.475370 0.167350  
0.479450 0.167350  
0.483530 0.167350  
0.487610 0.167350  
0.491690 0.167350  
0.495770 0.167350  
0.499850 0.167350  
0.503930 0.167350  
0.508010 0.167350  
0.512090 0.167350  
0.516170 0.167350  
0.520250 0.167350  
0.524330 0.167350  
0.528410 0.167350  
0.532490 0.167350  
0.536570 0.167350  
0.540650 0.167350  
0.544730 0.167350  
0.548810 0.167350  
0.552890 0.167350  
0.556970 0.167350  
0.561050 0.167350  
0.565130 0.167350  
0.569210 0.167350  
0.573290 0.167350  
0.577370 0.167350  
0.581450 0.167350  
0.585530 0.167350  
0.589610 0.167350  
0.593690 0.167350  
0.597770 0.167350  
0.601850 0.167350  
0.605930 0.167350  
0.610010 0.167350  
0.614090 0.167350  
0.618170 0.167350  
0.622250 0.167350  
0.626330 0.167350  
0.630410 0.167350  
0.634490 0.167350  
0.638570 0.167350  
0.642650 0.167350  
0.646730 0.167350  
0.650810 0.167350  
0.654890 0.167350  
0.658970 0.167350  
0.663050 0.167350  
0.667130 0.167350  
0.671210 0.167350  
0.675290 0.167350  
0.679370 0.167350  
0.683450 0.167350  
0.687530 0.167350  
0.691610 0.167350  
0.695690 0.167350  
0.699770 0.167350  
0.703850 0.167350  
0.707930 0.167350  
0.712010 0.167350  
0.716090 0.167350  
0.720170 0.167350  
0.724250 0.167350  
0.728330 0.167350  
0.732410 0.167350  
0.736490 0.167350  
0.740570 0.167350  
0.744650 0.167350  
0.748730 0.167350  
0.752810 0.167350  
0.756890 0.167350  
0.760970 0.167350  
0.765050 0.167350  
0.769130 0.167350  
0.773210 0.167350  
0.777290 0.167350  
0.781370 0.167350  
0.785450 0.167350  
0.789530 0.167350  
0.793610 0.167350  
0.797690 0.167350  
0.801770 0.167350  
0.805850 0.167350  
0.809930 0.167350  
0.814010 0.167350  
0.818090 0.167350  
0.822170 0.167350  
0.826250 0.167350  
0.830330 0.167350  
0.834410 0.167350  
0.838490 0.167350  
0.842570 0.167350  
0.846650 0.167350  
0.850730 0.167350  
0.854810 0.167350  
0.858890 0.167350  
0.862970 0.167350  
0.867050 0.167350  
0.871130 0.167350  
0.875210 0.167350  
0.879290 0.167350  
0.883370 0.167350  
0.887450 0.167350  
0.891530 0.167350  
0.895610 0.167350  
0.899690 0.167350  
0.903770 0.167350  
0.907850 0.167350  
0.911930 0.167350  
0.916010 0.167350  
0.920090 0.167350  
0.924170 0.167350  
0.928250 0.167350  
0.932330 0.167350  
0.936410 0.167350  
0.940490 0.167350  
0.944570 0.167350  
0.948650 0.167350  
0.952730 0.167350  
0.956810 0.167350  
0.960890 0.167350  
0.964970 0.167350  
0.969050 0.167350  
0.973130 0.167350  
0.977210 0.167350  
0.981290 0.167350  
0.985370 0.167350  
0.989450 0.167350  
0.993530 0.167350  
0.997610 0.167350  
1.001690 0.167350  
1.005770 0.167350  
1.009850 0.167350  
1.013930 0.167350  
1.018010 0.167350  
1.022090 0.167350  
1.026170 0.167350  
1.030250 0.167350  
1.034330 0.167350  
1.038410 0.167350  
1.042490 0.167350  
1.046570 0.167350  
1.050650 0.167350  
1.054730 0.167350  
1.058810 0.167350  
1.062890 0.167350  
1.066970 0.167350  
1.071050 0.167350  
1.075130 0.167350  
1.079210 0.167350  
1.083290 0.167350  
1.087370 0.167350  
1.091450 0.167350  
1.095530 0.167350  
1.099610 0.167350  
1.103690 0.167350  
1.107770 0.167350  
1.111850 0.167350  
1.115930 0.167350  
1.119970 0.167350  
1.124050 0.167350  
1.128130 0.167350  
1.132210 0.167350  
1.136290 0.167350  
1.140370 0.167350  
1.144450 0.167350  
1.148530 0.167350  
1.152610 0.167350  
1.156690 0.167350  
1.160770 0.167350  
1.164850 0.167350  
1.168930 0.167350  
1.173010 0.167350  
1.177090 0.167350  
1.181170 0.167350  
1.185250 0.167350  
1.189330 0.167350  
1.193410 0.167350  
1.197490 0.167350  
1.201570 0.167350  
1.205650 0.167350  
1.209730 0.167350  
1.213810 0.167350  
1.217890 0.167350  
1.221970 0.167350  
1.226050 0.167350  
1.230130 0.167350  
1.234210 0.167350  
1.238290 0.167350  
1.242370 0.167350  
1.246450 0.167350  
1.250530 0.167350  
1.254610 0.167350  
1.258690 0.167350  
1.262770 0.167350  
1.266850 0.167350  
1.270930 0.167350  
1.275010 0.167350  
1.279090 0.167350  
1.283170 0.167350  
1.287250 0.167350  
1.291330 0.167350  
1.295410 0.167350  
1.299490 0.167350  
1.303570 0.167350  
1.307650 0.167350  
1.311730 0.167350  
1.315810 0.167350  
1.319890 0.167350  
1.323970 0.167350  
1.328050 0.167350  
1.332130 0.167350  
1.336210 0.167350  
1.340290 0.167350  
1.344370 0.167350  
1.348450 0.167350  
1.352530 0.167350  
1.356610 0.167350  
1.360690 0.167350  
1.364770 0.167350  
1.368850 0.167350  
1.372930 0.167350  
1.377010 0.167350  
1.381090 0.167350  
1.385170 0.167350  
1.389250 0.167350  
1.393330 0.167350  
1.397410 0.167350  
1.401490 0.167350  
1.405570 0.167350  
1.409650 0.167350  
1.413730 0.167350  
1.417810 0.167350  
1.421890 0.167350  
1.425970 0.167350  
1.430050 0.167350  
1.434130 0.167350  
1.438210 0.167350  
1.442290 0.167350  
1.446370 0.167350  
1.450450 0.167350  
1.454530 0.167350  
1.458610 0.167350  
1.462690 0.167350  
1.466770 0.167350  
1.470850 0.167350  
1.474930 0.167350  
1.479010 0.167350  
1.483090 0.167350  
1.487170 0.167350  
1.491250 0.167350  
1.495330 0.167350  
1.499410 0.167350  
1.503490 0.167350  
1.507570 0.167350  
1.511650 0.167350  
1.515730 0.167350  
1.519810 0.167350  
1.523890 0.167350  
1.527970 0.167350  
1.532050 0.167350  
1.536130 0.167350  
1.540210 0.167350  
1.544290 0.167350  
1.548370 0.167350  
1.552450 0.167350  
1.556530 0.167350  
1.560610 0.167350  
1.564690 0.167350  
1.568770 0.167350  
1.572850 0.167350  
1.576930 0.167350  
1.581010 0.167350  
1.585090 0.167350  
1.589170 0.167350  
1.593250 0.167350  
1.597330 0.167350  
1.601410 0.167350  
1.605490 0.167350  
1.609570 0.167350  
1.613650 0.167350  
1.617730 0.167350  
1.621810 0.167350  
1.625890 0.167350  
1.629970 0.167350  
1.634050 0.167350  
1.638130 0.167350  
1.642210 0.167350  
1.646290 0.167350  
1.650370 0.167350  
1.654450 0.167350  
1.658530 0.167350  
1.662610 0.167350  
1.666690 0.167350  
1.670770 0.167350  
1.674850 0.167350  
1.678930 0.167350  
1.683010 0.167350  
1.687090 0.167350  
1.691170 0.167350  
1.695250 0.167350  
1.699330 0.167350  
1.703410 0.167350  
1.707490 0.167350  
1.711570 0.167350  
1.715650 0.167350  
1.719730 0.167350  
1.723810 0.167350  
1.727890 0.167350  
1.731970 0.167350  
1.736050 0.167350  
1.740130 0.167350  
1.744210 0.167350  
1.748290 0.167350  
1.752370 0.167350  
1.756450 0.167350  
1.760530 0.167350  
1.764610 0.167350  
1.768690 0.167350  
1.772770 0.167350  
1.776850 0.167350  
1.780930 0.167350  
1.785010 0.167350  
1.789090 0.167350  
1.793170 0.167350  
1.797250 0.167350  
1.801330 0.167350  
1.805410 0.167350  
1.809490 0.167350  
1.813570 0.167350  
1.817650 0.167350  
1.821730 0.167350  
1.825810 0.167350  
1.829890 0.167350  
1.833970 0.167350  
1.838050 0.167350  
1.842130 0.167350  
1.846210 0.167350  
1.850290 0.167350  
1.854370 0.167350  
1.858450 0.167350  
1.862530 0.167350  
1.866610 0.167350  
1.870690 0.167350  
1.874770 0.167350  
1.878850 0.167350  
1.882930 0.167350  
1.887010 0.167350  
1.891090 0.167350  
1.895170 0.167350  
1.899250 0.167350  
1.903330 0.167350  
1.907410 0.167350  
1.911490 0.167350  
1.915570 0.167350  
1.919650 0.167350  
1.923730 0.167350  
1.927810 0.167350  
1.931890 0.167350  
1.935970 0.167350  
1.940050 0.167350  
1.944130 0.167350  
1.948210 0.167350  
1.952290 0.167350  
1.956370 0.167350  
1.960450 0.167350  
1.964530 0.167350  
1.968610 0.167350  
1.972690 0.167350  
1.976770 0.167350  
1.980850 0.167350  
1.984930 0.167350  
1.989010 0.167350  
1.993090 0.167350  
1.997170 0.167350  
2.001250 0.167350  
2.005330 0.167350  
2.009410 0.167350  
2.013490 0.167350  
2.017570 0.167350  
2.021650 0.167350  
2.025730 0.167350  
2.029810 0.167350  
2.033890 0.167350  
2.037970 0.167350  
2.042050 0.167350  
2.046130 0.167350  
2.050210 0.167350  
2.054290 0.167350  
2.058370 0.167350  
2.062450 0.167350  
2.066530 0.167350  
2.070610 0.167350  
2.074690 0.167350  
2.078770 0.167350  
2.082850 0.167350  
2.086930 0.167350  
2.091010 0.167350  
2.095090 0.167350  
2.099170 0.167350  
2.103250 0.167350  
2.107330 0.167350  
2.111410 0.167350  
2.115490 0.167350  
2.119570 0.167350  
2.123650 0.167350  
2.127730 0.167350  
2.131810 0.167350  
2.135890 0.167350  
2.139970 0.167350  
2.144050 0.167350  
2.148130 0.167350  
2.152210 0.167350  
2.156290 0.167350  
2.160370 0.167350  
2.164450 0.167350  
2.168530 0.167350  
2.172610 0.167350  
2.176690 0.167350  
2.180770 0.167350  
2.184850 0.167350  
2.188930 0.167350  
2.193010 0.167350  
2.197090 0.167350  
2.201170 0.167350  
2.205250 0.167350  
2.209330 0.167350  
2.213410 0.167350  
2.217490 0.167350  
2.221570 0.167350  
2.225650 0.167350  
2.229730 0.167350  
2.233810 0.167350  
2.237890 0.167350  
2.241970 0.167350  
2.246050 0.167350  
2.250130 0.167350  
2.254210 0.167350  
2.258290 0.167350  
2.262370 0.167350  
2.266450 0.167350  
2.270530 0.167350  
2.274610 0.167350  
2.278690 0.167350  
2.282770 0.167350  
2.286850 0.167350  
2.290930 0.167350  
2.295010 0.167350  
2.299090 0.167350  
2.303170 0.167350  
2.307250 0.167350  
2.311330 0.167350  
2.315410 0.167350  
2.319490 0.167350  
2.323570 0.167350  
2.327650 0.167350  
2.331730 0.167350  
2.335810 0.167350  
2.339890 0.167350  
2.343970 0.167350  
2.348050 0.167350  
2.352130 0.167350  
2.356210 0.167350  
2.360290 0.167350  
2.364370 0.167350  
2.368450 0.167350  
2.372530 0.167350  
2.376610 0.167350  
2.380690 0.167350  
2.384770 0.167350  
2.388850 0.167350  
2.392930 0.167350  
2.397010 0.167350  
2.401090 0.167350  
2.405170 0.167350  
2.409250 0.167350  
2.413330 0.167350  
2.417410 0.167350  
2.421490 0.167350  
2.425570 0.167350  
2.429650 0.167350  
2.433730 0.167350  
2.437810 0.167350  
2.441890 0.167350  
2.445970 0.167350  
2.450050 0.167350  
2.454130 0.167350  
2.458210 0.167350  
2.462290 0.167350  
2.466370 0.167350  
2.470450 0.167350  
2.474530 0.167350  
2.478610 0.167350  
2.482690 0.167350  
2.486770 0.167350  
2.490850 0.167350  
2.494930 0.167350  
2.499010 0.167350  
2.503090 0.167350  
2.507170 0.167350  
2.511250 0.167350  
2.515330

## References

[illegible]

0.512758 0.018750 0.000816 0.613112 0.018001 0.000714  
0.712159 0.016244 0.000767 0.809952 0.013006 0.000882  
0.858097 0.010985 0.001014 0.905906 0.008316 0.001066  
0.953199 0.005029 0.000962 0.976692 0.002804 0.000536  
0.981325 0.002381 0.000455 0.986046 0.001845 0.000295  
0.990670 0.001328 0.000214 0.999972 0.000248 -0.000042  
1.000000 0.000000 0.000000  
0.50000 -11.06788 0.11404 0.00649 0.07303  
0.000000 0.000000 0.000000 0.000579 0.000363 -0.001332  
0.011294 0.001983 -0.001218 0.016726 0.002518 -0.001215  
0.022183 0.003007 -0.001291 0.027472 0.003525 -0.001188  
0.054597 0.003127 -0.001109 0.108255 0.007495 -0.001094  
0.161500 0.009257 -0.001021 0.214373 0.010475 -0.000948  
0.319187 0.011932 -0.001178 0.422586 0.012306 -0.001527  
0.524057 0.012176 -0.001575 0.623666 0.011470 -0.001857  
0.721121 0.010139 -0.001557 0.816396 0.008090 -0.001045  
0.863262 0.006645 -0.000645 0.909419 0.005087 -0.000257  
0.955000 0.003123 0.000118 0.977556 0.001787 0.000141  
0.982078 0.001433 0.000067 0.986512 0.001224 0.000072  
0.990927 0.000978 0.000069 0.999972 0.000200 -0.000007  
1.000000 0.000000 0.000000  
0.13265 16.00513 -0.07960 -0.00140 0.14266  
0.000000 0.000000 0.000000 0.000839 0.002442 -0.002672  
0.011218 0.010592 -0.009631 0.015532 0.013069 -0.011570  
0.021843 0.014997 -0.012987 0.027166 0.016947 -0.014461  
0.053694 0.023720 -0.018931 0.106481 0.034961 -0.025740  
0.158762 0.044046 -0.030718 0.210443 0.051772 -0.034709  
0.311382 0.064180 -0.040684 0.408164 0.072636 -0.044692  
0.503382 0.075556 -0.046687 0.604113 0.071475 -0.045205  
0.708829 0.062111 -0.039261 0.807796 0.047456 -0.029540  
0.854945 0.037700 -0.023489 0.902278 0.026537 -0.016731  
0.950749 0.014131 -0.009044 0.975293 0.007226 -0.004624  
0.980209 0.005863 -0.003774 0.985139 0.004500 -0.002930  
0.990055 0.003138 -0.002080 0.999873 0.000441 -0.000400  
1.000000 0.000000 0.000000  
0.15306 14.58914 -0.08970 -0.00144 0.14551  
0.000000 0.000000 0.000000 0.000736 0.001909 -0.002150  
0.010961 0.008590 -0.007520 0.016177 0.010670 -0.008983  
0.021417 0.012261 -0.009998 0.026622 0.013886 -0.011088  
0.052722 0.019569 -0.014099 0.104729 0.028833 -0.018503  
0.156501 0.036044 -0.021457 0.208050 0.041928 -0.023695  
0.310444 0.050551 -0.026809 0.411894 0.055436 -0.028598  
0.512352 0.056283 -0.028683 0.611759 0.052427 -0.026307  
0.710056 0.044733 -0.021845 0.807342 0.032686 -0.015351  
0.855676 0.023460 -0.011555 0.903865 0.017616 -0.007705  
0.951931 0.009167 -0.003881 0.975952 0.004633 -0.001870  
0.980764 0.003756 -0.001502 0.985556 0.002859 -0.001161  
0.990365 0.001982 -0.000821 0.999884 0.000270 -0.000158  
1.000000 0.000000 0.000000  
0.16327 13.87381 -0.09412 -0.00149 0.14719  
0.000000 0.000000 0.000000 0.000725 0.001762 -0.002030  
0.010910 0.008154 -0.007071 0.016118 0.010139 -0.008428  
0.021332 0.011667 -0.009389 0.026529 0.013202 -0.010376  
0.052525 0.018635 -0.013107 0.104379 0.027455 -0.017020  
0.155998 0.034246 -0.019584 0.207425 0.039690 -0.021386  
0.309677 0.047439 -0.023654 0.411086 0.051456 -0.024522  
0.511649 0.051552 -0.023714 0.611339 0.047282 -0.020773  
0.710106 0.039375 -0.016369 0.807871 0.028438 -0.011068  
0.856338 0.022091 -0.008280 0.904536 0.015279 -0.005417  
0.952402 0.007989 -0.002864 0.976223 0.004036 -0.001417  
0.980965 0.003258 -0.001139 0.985733 0.002500 -0.000896  
0.990470 0.001722 -0.000645 0.999942 0.000193 -0.000196  
1.000000 0.000000 0.000000  
0.18367 12.42068 -0.10184 -0.00170 0.15075  
0.000000 0.000000 0.000000 0.000666 0.001459 -0.001728  
0.010822 0.007145 -0.006124 0.016011 0.008912 -0.007254  
0.021193 0.010284 -0.008043 0.026384 0.011682 -0.008891  
0.052249 0.016603 -0.011092 0.103853 0.024682 -0.014196  
0.155244 0.030938 -0.016167 0.206434 0.035986 -0.017519  
0.308232 0.043098 -0.019181 0.409270 0.046739 -0.019747  
0.509554 0.046704 -0.018875 0.609115 0.042625 -0.016185  
0.707949 0.035256 -0.012261 0.806049 0.025213 -0.007770  
0.854822 0.019415 -0.005572 0.903401 0.013336 -0.003543  
0.951790 0.006872 -0.001752 0.975908 0.003462 -0.000859  
0.980741 0.002773 -0.000707 0.985552 0.002118 -0.000548  
0.990359 0.001463 -0.000415 0.999985 0.000153 -0.000156  
1.000000 0.000000 0.000000  
0.20408 11.06547 -0.10851 -0.00209 0.15466



## REFERENCES

1. Adamczyk, J.J.: Model Equation for Simulating Flows in Multistage Turbomachinery. ASME Paper 85-GT-226, Mar. 1985 (NASA TM-86869).
2. Thompson, J.F., Warsi, Z.U.A., and Mastin, C.W.: Numerical Grid Generation: Foundations and Applications. Elsevier Science Publishing Co., 1985.
3. Faux, I.D., and Pratt, M.A.: Computational Geometry for Design and Manufacture. Ellis Horwood Ltd., 1979.
4. Bober, L.J., Chaussee, D.S., and Kutler, P.: Prediction of High Speed Propeller Flow Fields Using a Three-Dimensional Euler Analysis. AIAA Paper 83-0188, Jan. 1983 (NASA TM-83065).
5. Denton, J.D.: Time Marching Methods for Turbomachinery Flow Calculations. Numerical Methods in Applied Fluid Dynamics, B. Hunt, ed., Academic Press, New York, 1980, pp. 473-493.



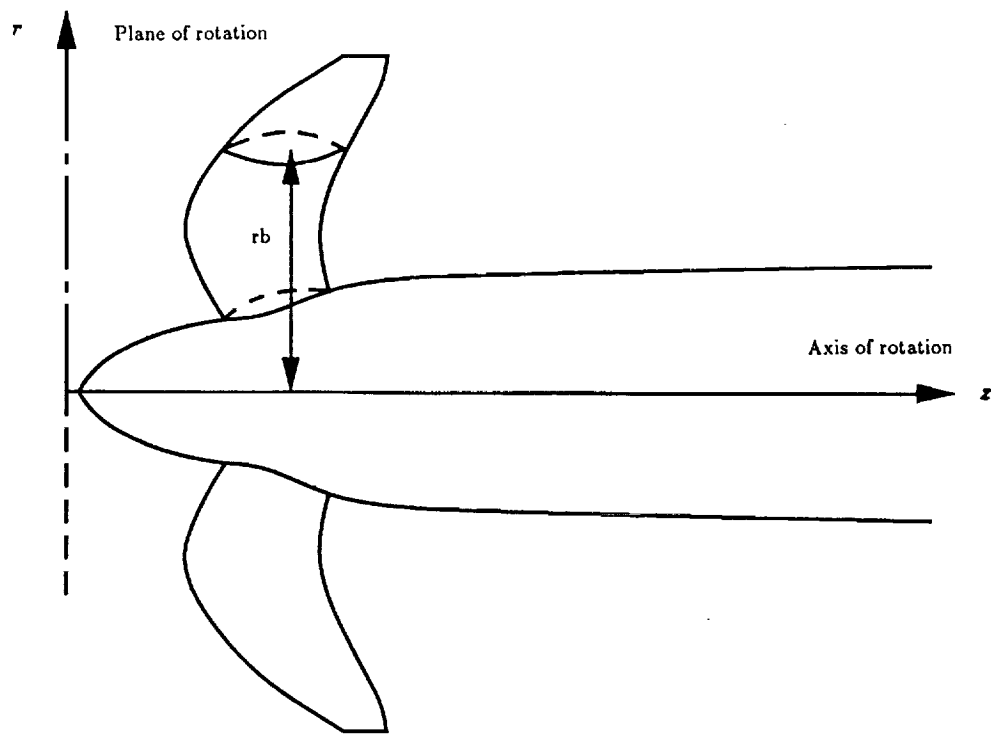


Figure 1. - Description of nacelle and blade geometries.

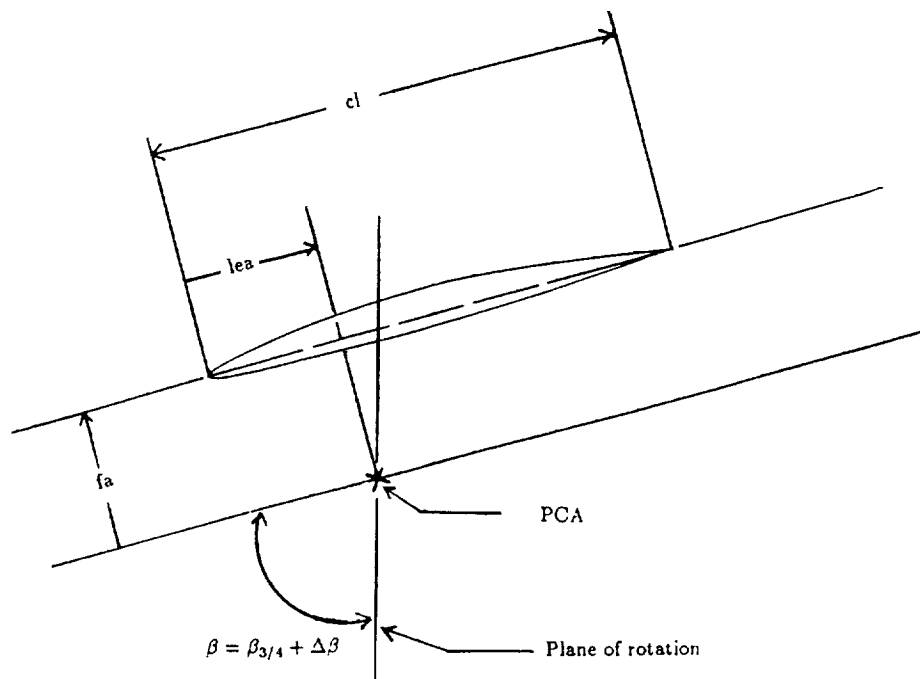


Figure 2. - Description of sectional blade geometry.

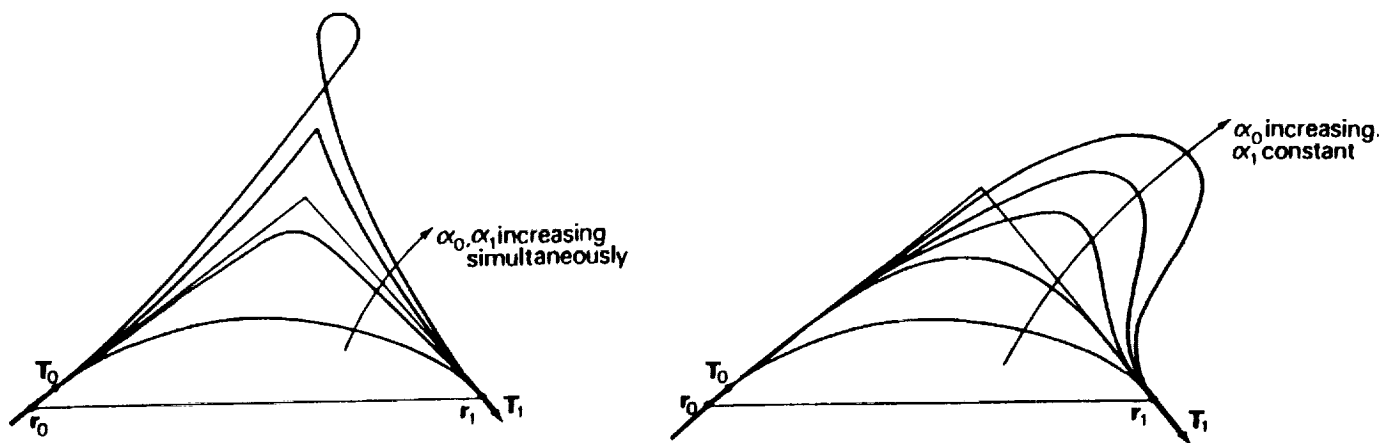


Figure 3. - Effect of tangent vector lengths on shape of Ferguson cubic curves.

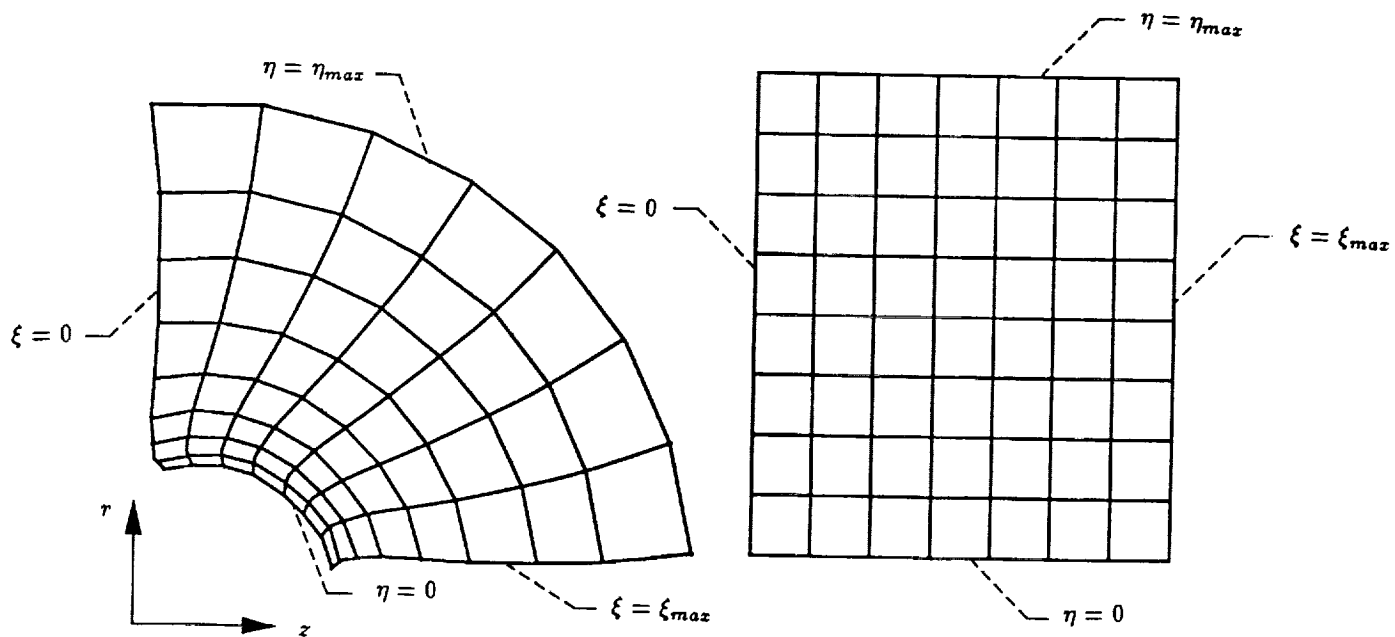


Figure 4. - Physical and computational planes.

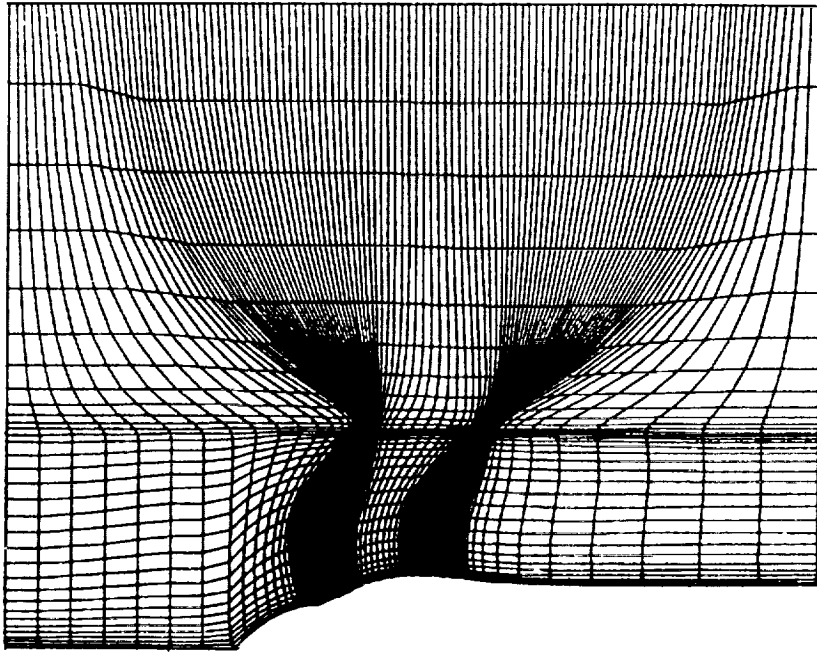
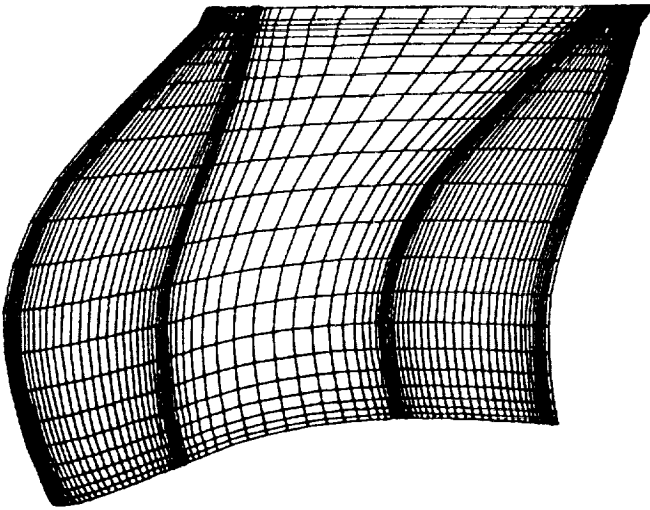
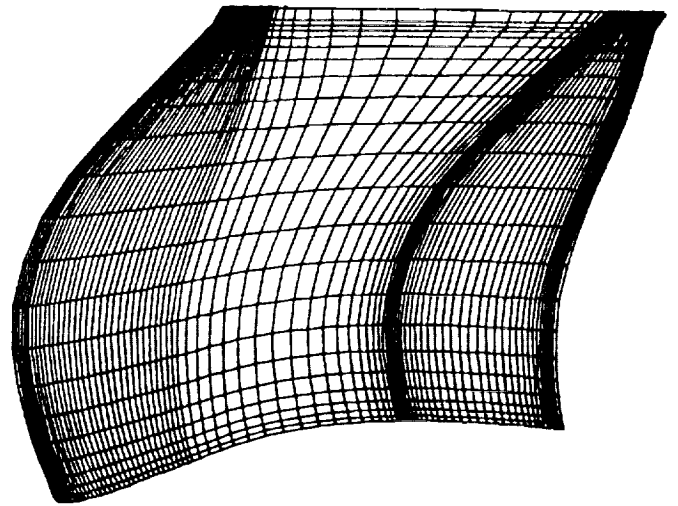


Figure 5. -  $z - r$  plane of counterrotation H-mesh.



(a)  $DZTE = 0.5$



(b)  $DZTE = 1.0$

Figure 6 - Effect of clustering factors on blade point distribution.

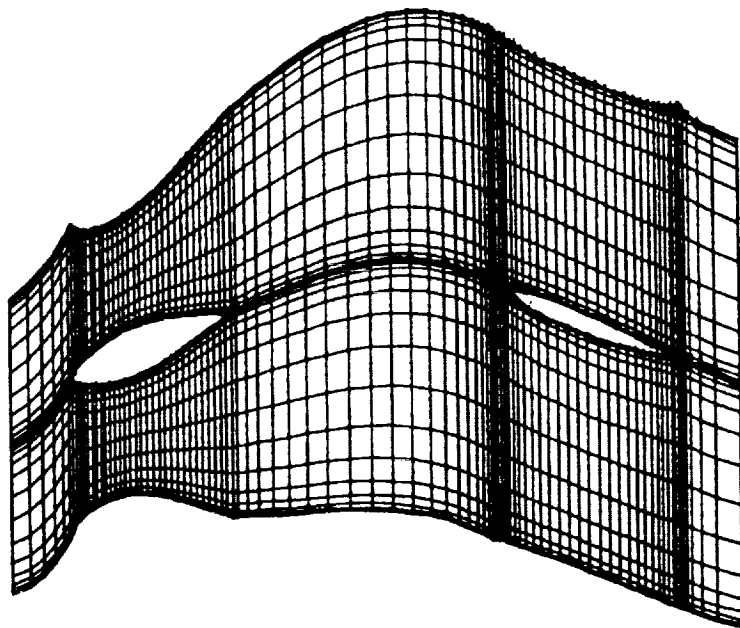
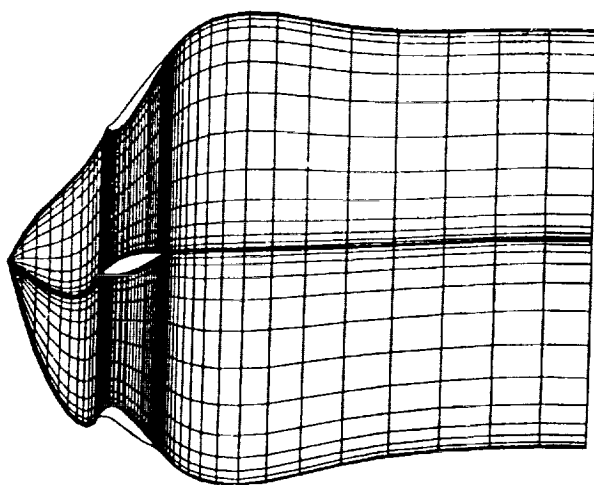
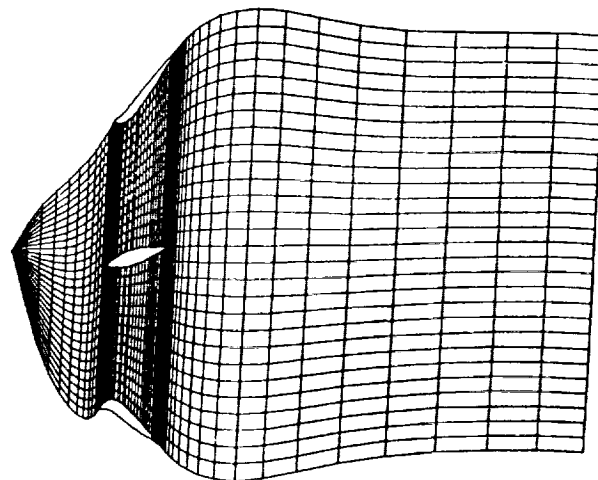


Figure 7. - Constant radial cut at hub (counterrotation case).

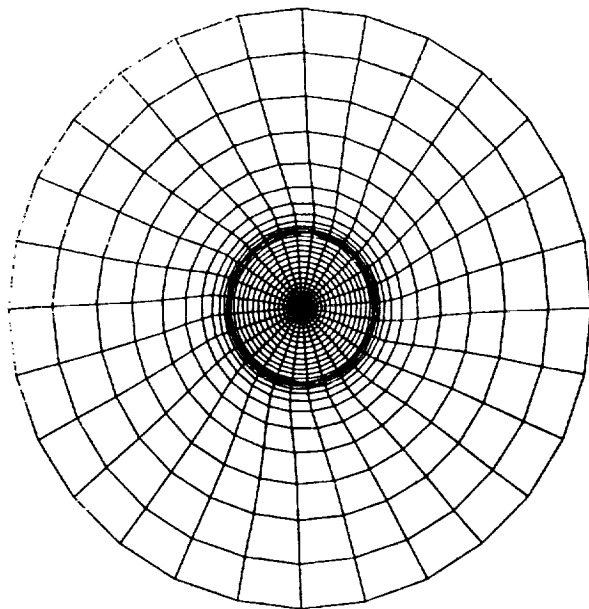


(a)  $DTHBL = 0.1$

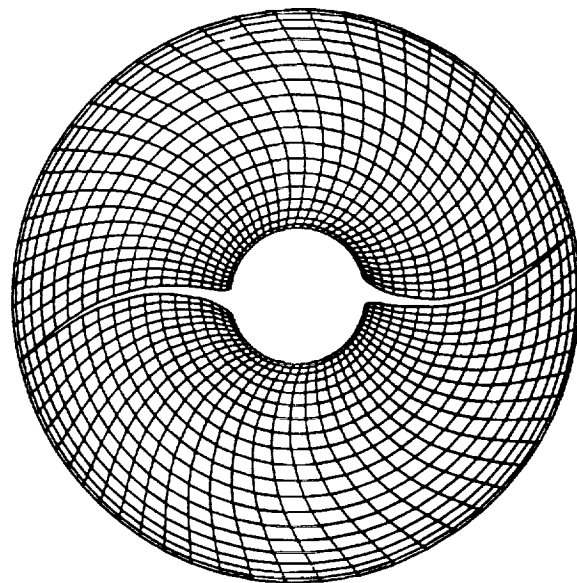


(b)  $DTHBL = 1.0$

Figure 8. - Effect of DTHBL on circumferential point distribution.



(a) At inlet.



(b) At midchord.

Figure 9. - Constant axial cut.

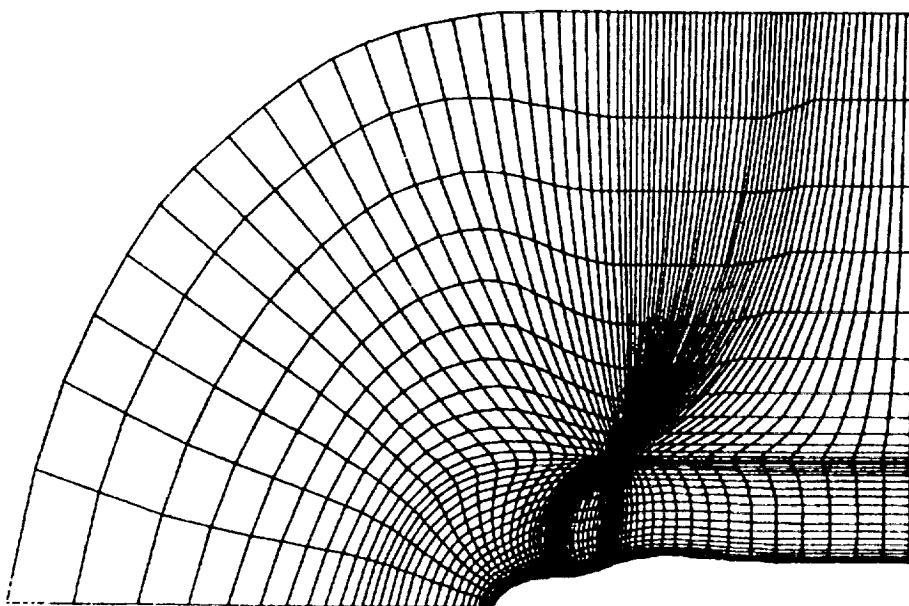
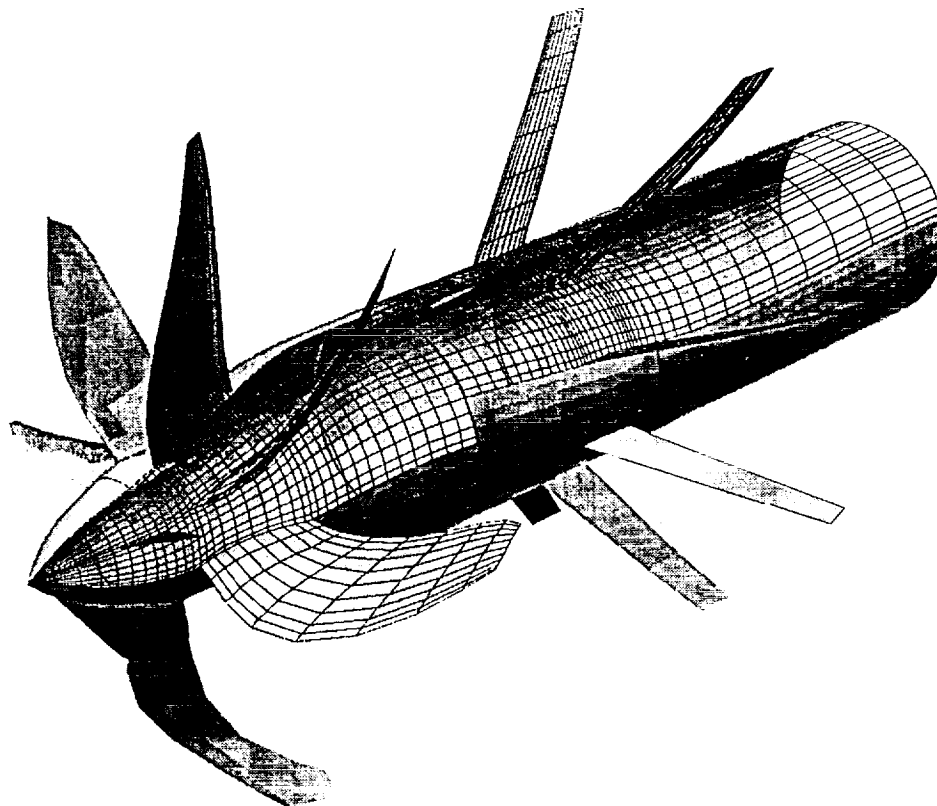
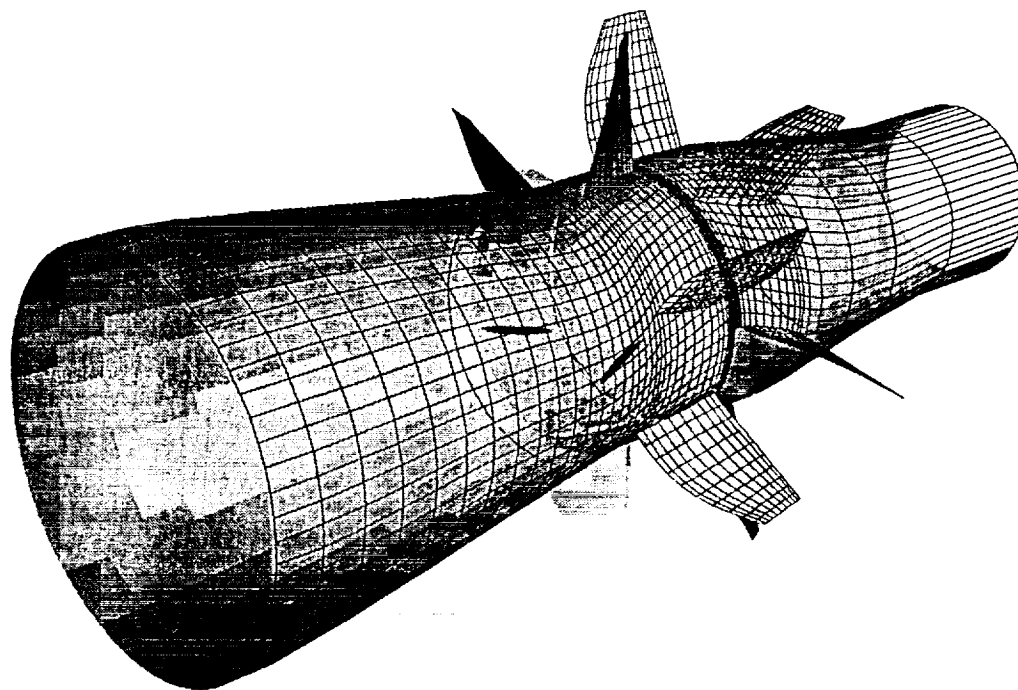


Figure 10. -  $z - r$  plane of typical C-mesh.

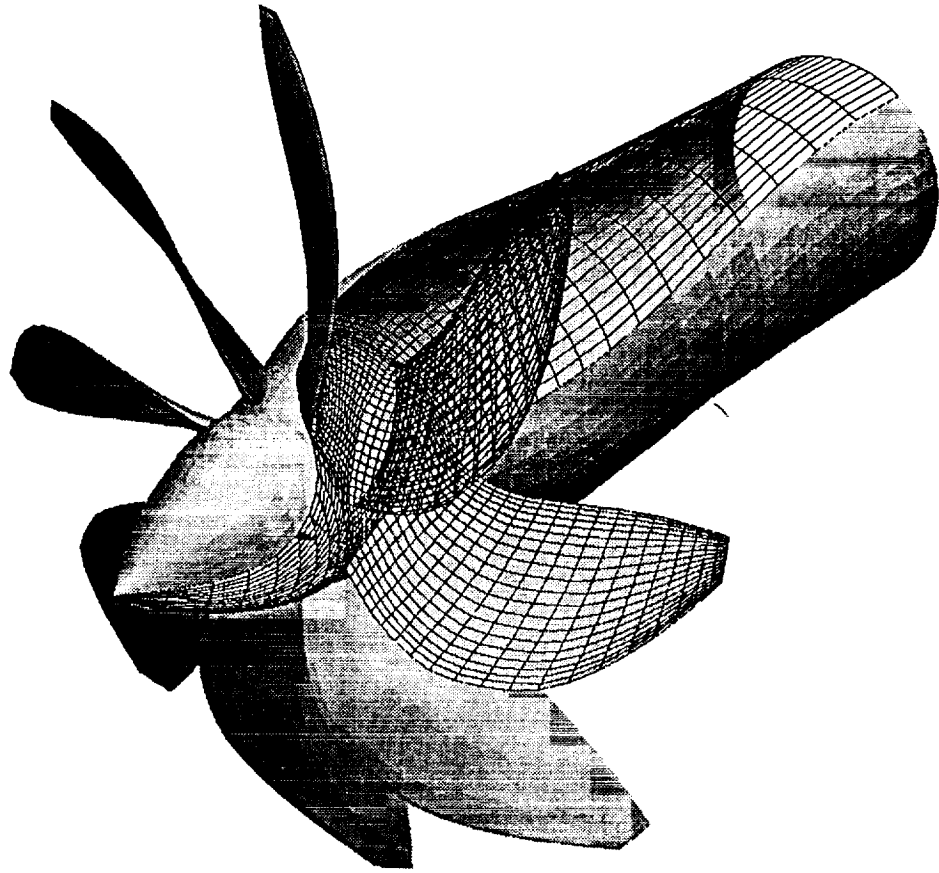


(a) Swirl-recovery vane (SRV)



(b) Cruise missile (CM)

Figure 11. - Surface grids.



(c) Advanced turboprop (ATP)

Figure 11. - Concluded.

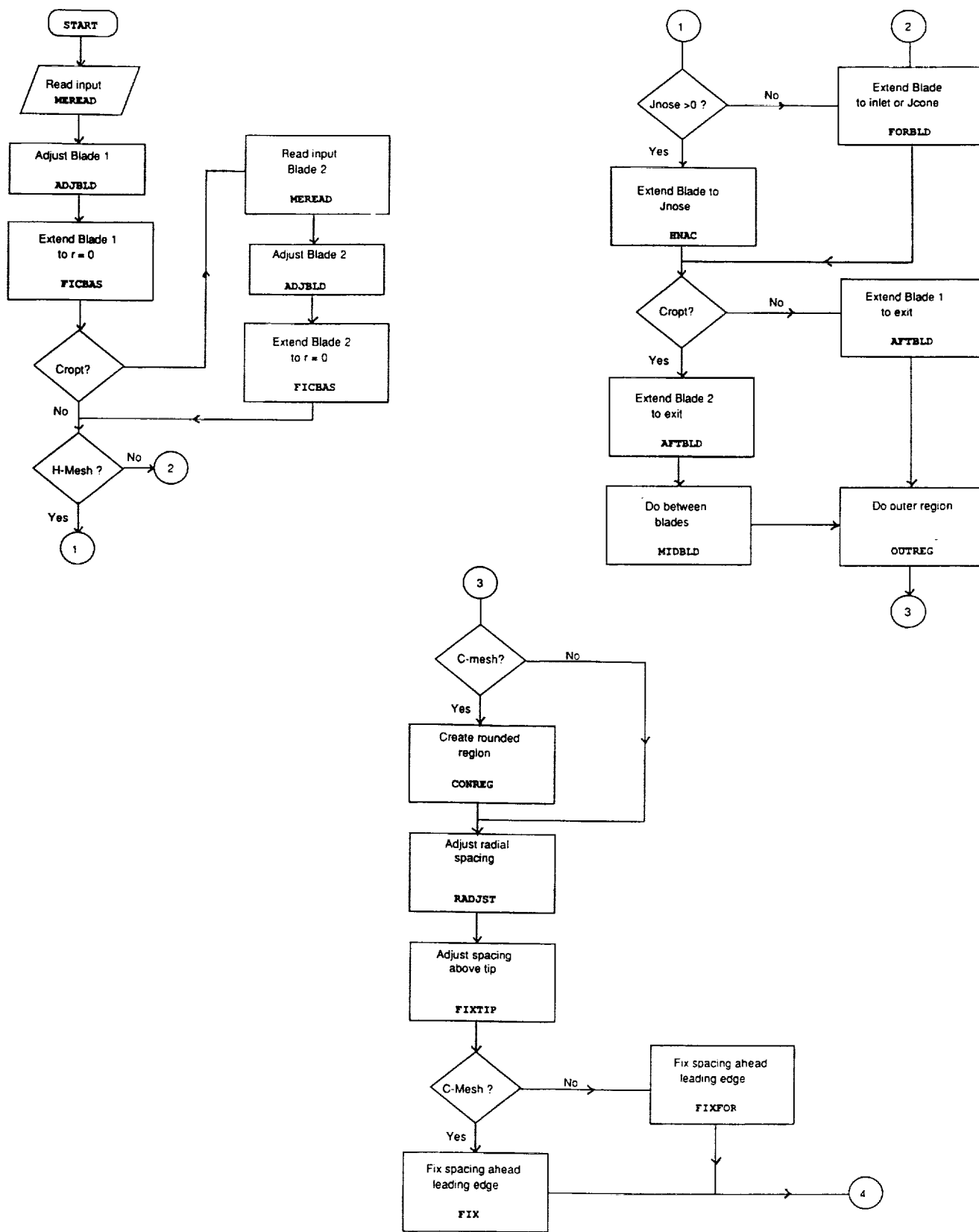


Figure 12. - Flow chart of main program structure.



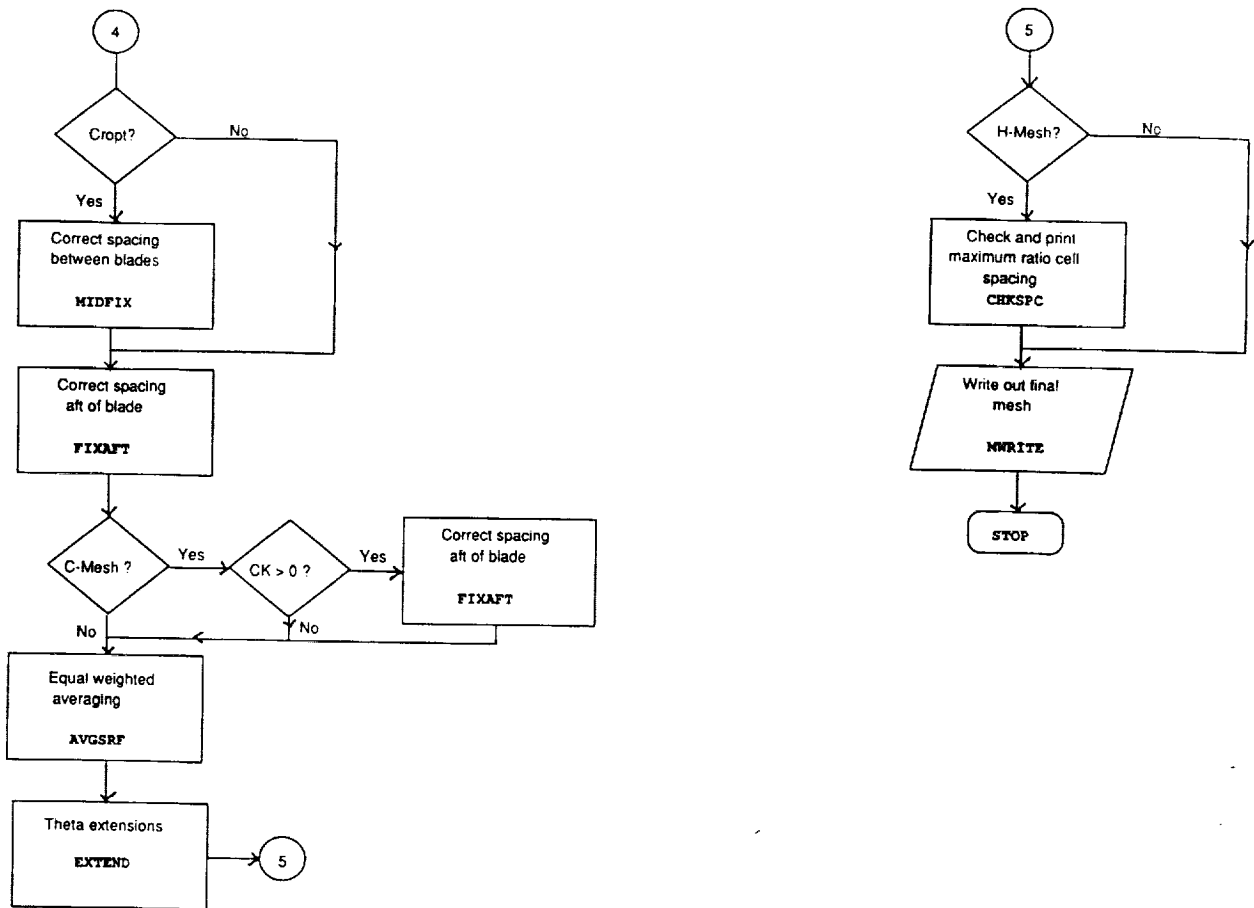


Figure 12 - Concluded.



National Aeronautics and  
Space Administration

## Report Documentation Page

1. Report No. NASA CR-185156	2. Government Accession No.	3. Recipient's Catalog No.	
4. Title and Subtitle User's Guide to PMESH—A Grid-Generation Program for Single-Rotation and Counterrotation Advanced Turboprops		5. Report Date December 1989	
		6. Performing Organization Code	
7. Author(s) Saif A. Warsi		8. Performing Organization Report No. None (E-5152)	
		10. Work Unit No. 535-05-01	
9. Performing Organization Name and Address Sverdrup Technology, Inc. NASA Lewis Research Center Group Cleveland, Ohio 44135		11. Contract or Grant No. NAS3-24105	
		13. Type of Report and Period Covered Contractor Report Final	
12. Sponsoring Agency Name and Address National Aeronautics and Space Administration Lewis Research Center Cleveland, Ohio 44135-3191		14. Sponsoring Agency Code	
15. Supplementary Notes Project Manager, Lawrence J. Bober, Propulsion Systems Division, NASA Lewis Research Center.			
16. Abstract <p>This report presents a detailed operating manual for a grid-generation program that produces three-dimensional meshes for advanced turboprops. The code uses both algebraic and elliptic partial differential equation (PDE) methods to generate single-rotation and counterrotation, H- or C-type meshes for the <math>z - r</math> planes and H-type for the <math>z - \theta</math> planes. The code allows easy specification of geometrical constraints (such as blade angle, location of bounding surfaces, etc.), mesh control parameters (point distribution near blades and nacelle, number of grid points desired, etc.), and it has good runtime diagnostics. This report provides an overview of the mesh-generation procedure, sample input dataset with detailed explanation of all input, and example meshes.</p>			
17. Key Words (Suggested by Author(s)) Mesh generator Propeller Propfan		18. Distribution Statement Unclassified—Unlimited Subject Category 02	
19. Security Classif. (of this report) Unclassified	20. Security Classif. (of this page) Unclassified	21. No. of pages 24	22. Price* A02